Journal of Oil Palm Research Vol. 35 (4) December 2023 p. 713-724
DOI: https://doi.org/10.21894/jopr.2023.0020

LINEAR KINETICS MODELLING AND THERMODYNAMICS STUDY OF SUPERCRITICAL CO_2-DERIVED OIL EXTRACTS FROM PALM FRUIT MESOCARP

USMAN BELLO[1]; NURUL AINI AMRAN[1,2]*; SHAFIRAH SAMSURI[1,2] and MUHAMMAD SYAFIQ HAZWAN RUSLAN[3]

ABSTRACT

Supercritical fluid extraction (SFE) is a green processing technique that employed the use of carbon dioxide (CO_2) as an extractant in place of organic or inorganic solvents. In this study, SFE was used to recover oil from the milled palm fruit peels as a sustainable feedstock. The process was carried out at five different temperatures of 40°C-80°C, varied extraction time of 30-150 min, a fixed pressure of 25 MPa, a flow rate of 5 mL min^{-1}, and a co-solvent ratio of 5.00% vol. The result shows that an optimum extract yield of 3.95% was recovered at the maximum temperature (80°C) after 150 min. The experimentally obtained data were subjected to kinetic analysis using Elovich's, Hyperbolic and Pseudo second-order models. Models' suitability to the data fitness was tested using seven error functions, in which Elovich's was found to be the best-fitted model, succeeded by the Hyperbolic and then Pseudo second-order. Also, the result of statistical analysis using ANOVA, indicates that temperature has more impact on improving the rate of extract recovery than extraction time. Finally, the thermodynamic studies revealed that an irreversible and endothermically forward reaction was observed considering the values of the entropy change (ΔS) = 0.138 J mol^{-1} K^{-1}, enthalpy change (ΔH) = 53.50 K J mol^{-1}, and Gibbs' free energy, (ΔG) = -6.04 K J mol^{-1} respectively.

Keywords: kinetics, oil extracts, supercritical fluid extraction, thermodynamics study.

Received: 18 October 2022; **Accepted:** 22 February 2023; **Published online:** 3 May 2023.

INTRODUCTION

The palm fruit is noteworthy for its high concentration of various bioactive compounds, particularly carotenoids, which can be used as dietary supplements, antioxidants and other health-value promoting compounds (Aini *et al*., 2022). In Malaysia, the expansion of palm oil plantations and processing has been intensified, particularly in the forested areas of Borneo, Sumatra, and the Malay Peninsula, due to the significant economic importance of palm oil as a source of revenue through exports (Anuar *et al*., 2021; Meijaard *et al*., 2020). Palm oil is widely used to meet the global annual demand of 40% of vegetable oil for food, as well as in a variety of industrial processes, including pharmaceuticals, body care products and biofuel production (Mohajershojaei *et al*., 2015). However, the push towards finding suitable extraction techniques that are environmentally friendly, less time-consuming and economically viable, led to the transition from the use of conventional to non-conventional extraction techniques. Part of the reasons for this includes the relatively poor success recorded in the recovery of bioactive compounds

[1] Chemical Engineering Department, Universiti Teknologi PETRONAS, 32610 Seri Iskandar, Perak, Malaysia.

[2] HICoE - Centre for Biofuel and Biochemical Research (CBBR), Universiti Teknologi PETRONAS, 32610 Seri Iskandar, Perak, Malaysia.

[3] School of Chemical Engineering, College of Engineering, Universiti Teknologi MARA, 40450 Shah Alam, Selangor, Malaysia.

* *Corresponding author e-mail: nurul.amran@utp.edu.my*

from extracts derived using conventional extraction methods, coupled with high temperature and energy demand for the process (Chai *et al*., 2020).

The growing objections coming from chemical industries on the risk associated with hazardous solvents for extraction using conventional techniques have led to the increased popularity of non-conventional methods (Rodrigues *et al*., 2020). One such method is SFE, which is favoured for being a clean and green process that is non-polluting and toxic-free (Rodrigues *et al*., 2020). This has made SFE a promising extraction technique as it eliminates the drawbacks of conventional methods, such as long processing time, expensive solvents, high temperature, and high energy consumption (Miękus *et al*., 2019). Furthermore, the non-polar nature of the solvent used in SFE (CO_2) prevents oxidation, which can negatively impact the stability and potency of extracts obtained through traditional methods (Garcia-Mendoza *et al*., 2015). Additionally, the environmental-friendly nature of the extractant (CO_2) makes the SFE process more sustainable (Mohammad *et al*., 2007; Valdivia-Rivera *et al*., 2021). The solubilisation and mass transfer reaction of carotenoids from milled palm fruit peel to liquid extract is influenced by the similarity in polarity between the analyte and the extracting solvent (CO_2) (Mohammad *et al*., 2019).

The mechanism of the SFE process involves cooling the CO_2 in the reservoir to 0°C to enable it to be transferred into the reactor as a liquid. A polar modifier is added to increase the polarity of polar extractable compounds. Subsequently, the liquid CO_2 is then pumped into the extraction vessel which is kept at a temperature above its critical temperature (Chai *et al*., 2020). The pumping rate affects the fluid flow rate, and the pressure valve regulates the pressure. Thereafter, extracts are collected by releasing the collection pressure to atmospheric pressure (Miękus *et al*., 2019). However, the factors such as CO_2 flow rate, temperature, pressure and co-solvent ratio, are known to affect the extraction efficiency (Ruslan *et al*., 2018). On top of that, an increase in flow rate and temperature enhances diffusion rate and facilitates mass transfer reaction, thereby rupturing the plant cell wall and subsequent withdrawal of the bioactive compounds (Chanioti *et al*., 2021). Thus, an increase in pressure is proportional to the increase in yield theoretically, due to the growing solubility ratio, fluid density, solvating power of the Sc-CO_2, and increased solubility of the solute compounds (Yang *et al*., 2015).

Several kinetic models have been examined in studying the mass transfer reaction involving SFE in the literature (Patidar *et al*., 2022; Vélez-Erazo *et al*., 2021). However, a report on kinetic modelling of palm fruit extract derived from SFE using Elovich's, Hyperbolic and Pseudo second-order models are lacking to date. Kinetic modelling is crucial in engineering processes, as it helps understand the extraction mechanism and scale up the process for industrial use. This study aims to determine the suitability of these models in predicting mass transfer coefficients and identify the best-fit kinetic model for the extraction process. Effective modeling offers a deeper insight into the relationship between mass transfer reaction and solubility mechanism, leading to improved process design, reduced energy loss, and cost savings. The prediction of models' accuracy in fitting the experimental data was evaluated using seven statistical error functions (RMS, SEE, ARE%, SSE, HYBRID%, MPSED%, SD, and R^2). ANOVA was used to examine the impact of extraction time and temperature on extract rate and Tukey's *post hoc* HSD was used to compare the means. Additionally, the thermodynamic parameters ΔG, ΔH and ΔS of the extraction process were analysed.

EXPERIMENTAL

Supercritical Fluid Extraction (SFE)

Milled palm fruit peels were extracted using SFE according to a procedure reported by Ruslan *et al*. (2018). As presented in *Figure 1*, the 2D schematic assembled SFE setup comprises the solvent reservoir (CO_2 supply tank) supplying liquid chilled CO_2 (0°C) via conducting pipe to the extraction vessel inside the oven. The pumping rate normally controls the flow rate while pressure drop is controlled by the automated back pressure regulator, ABPR (Jasco, BP-2080 Plus). Extraction conditions for the significant SFE parameters used were a pressure of 25 MPa, a flow rate of 5 mL min^{-1}, and a co-solvent ratio of 5% vol. A 5 g of the milled palm fruit peel sample was loaded into the extraction vessel (Jasco, EV-3-50-2), and the time was noted after the first released pressure purge from the ABPR was completed. Subsequently, the oil extract was collected in an amber glass bottle immersed in an ice bath for 30, 60, 90, 120 and 150 min. Finally, the collected extracts were diluted with 2.0 mL of n-hexane and stored in a refrigerator at 4°C for HPLC analysis. Consequently, percentage yields recovered extracts were determined using Equation (1).

$$X_0\,(\%) = \frac{\text{Weight of extract obtained}}{\text{Weight of milled sample used}} \times 100 \quad (1)$$

Kinetic Studies

In this work, Elovich's, Hyperbolic, and Pseudo second-order models were explored in studying the kinetics of SFE for the recovered palm fruit extracts.

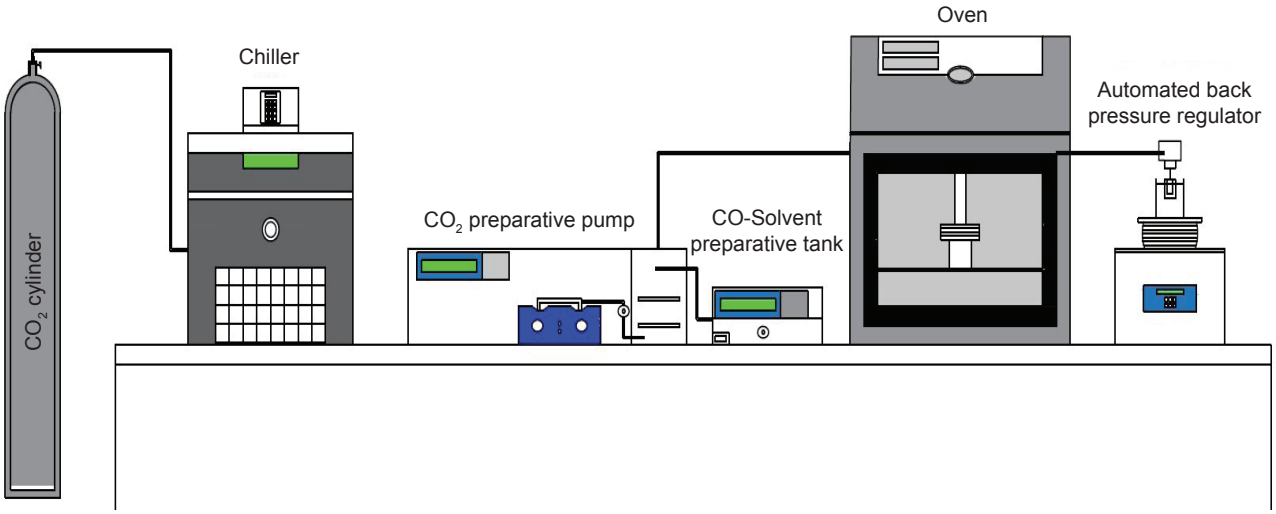

Figure 1. A schematic 2D diagram of SFE assembled setup.

TABLE 1. MODELS' DESCRIPTION FOR THE NON-LINEAR, LINEAR AND SLOPE-INTERCEPT FORMS

Kinetic models	Non-linear forms	Linear forms	Plots	Slopes	Intercepts
Elovich's model	$\frac{d\bar{q}}{dt} = \beta x + exp\,(-a\bar{q})$	$q = E_0 + E_1 \ln t$	q *vs* ln *t*	E_1	E_0
Hyperbolic model	$q = \frac{C_1 t}{1 + C_2 t}$	$\frac{1}{q} = \frac{1}{C_1} \times \frac{1}{t} + \frac{C_2}{C_1}$	$\frac{1}{q}$ *vs* $\frac{1}{t}$	$1/C_1$	C_2/C_1
Pseudo second-order model	$q = \frac{Cs^2 Kt}{1 + CsKt}$	$\frac{t}{Cs} = \frac{1}{KCs^2} + \frac{1}{Cs} t$	$\frac{t}{Cs}$ *vs* *t*	$1/C_s$	$\frac{1}{KCs^2}$

Note: C_1, C_2 - concentrations of extraction rate at the beginning and maximum extraction yield respectively; *Cs* - extraction capacity (g L^{-1}); *K* - extraction rate constant (L g^{-1} min^{-1}); E_0, E_1 - Elovich's parameters; *q* - extraction yield; *t* - time (min).

Table 1 presents the various expressions for the linear and non-linear forms of the study models, as well as their plots, slopes, and intercepts.

Elovich's model. This model established that an increment in the extraction yield is proportionally linked to a reduction in the extraction rate. As shown in the linear expression of this model (Equation 2), a plot of $\bar{q}$ against ln *t* gives the slope and intercepts as E_1 and E_0 respectively.

$$\bar{q} = E_0 + E_1 \ln t \tag{2}$$

Hyperbolic model. Using the linear form of this model is presented in Equation (3), a plot of 1/q against 1/t accounts for $1/C_1$ and C_2/C_1 as slope and intercept respectively.

$$\frac{1}{q} = \frac{1}{C_1} \times \frac{1}{t} + \frac{C_2}{C_1} \tag{3}$$

where the extraction yield is represented by $\bar{q}$, C_1 and C_2 are the initial rate and final extraction yield; and *t* is the extraction time.

Pseudo second-order model. Equation (4) represents the linear form of this model. From that, a plot of t/Cs against *t*, is plausible, with 1/Cs and $1/KCs^2$ as slope and intercept respectively.

$$\frac{t}{Ct} = \frac{1}{KCs^2} + \frac{1}{Cs} t \tag{4}$$

where *Cs* represent the extraction capacity, *Ct* is the fraction of extract yield after time *t* and *K* stands for the extraction rate constant.

Error Analysis

Seven error functions were utilised as statistical methods to determine the accuracy of the studied models in fitting the experimental data. This selection of variables was based on previous similar studies conducted by Riahi *et al*. (2017). Equations (5)-(12) were employed to calculate these error parameters.

$$R^2 = \frac{\sum_{N=1}^{N} (\bar{q}_{exp} + \bar{q}_{cal})^2}{\sum_{N=1}^{N} (\bar{q}_{exp} - \bar{q}_{cal})^2} \tag{5}$$

$$RMS = \sqrt{\frac{1}{N}\sum_{i=1}^{N}\left(\frac{\bar{q}_{exp} - \bar{q}_{cal}}{\bar{q}_{exp}}\right)^2} \quad (6)$$

$$SEE = \sqrt{\frac{\sum(x\text{-}y)^2}{dt}} \quad (7)$$

$$ARE\ \% = \frac{100}{N} \times \sum\left[\frac{|\bar{q}_{exp} - \bar{q}_{cal}|}{\bar{q}_{exp}}\right] \quad (8)$$

$$SSE = \sum(\bar{q}_{exp} - \bar{q}_{cal})^2 \quad (9)$$

$$HYBRID\ \% = \frac{1}{N-P}\sum\left[\frac{\bar{q}_{exp} - \bar{q}_{cal}}{\bar{q}_{exp}}\right]100 \quad (10)$$

$$MPSED\ \% = \sqrt{\frac{\sum\left[\frac{\bar{q}_{exp} - \bar{q}_{cal}}{\bar{q}_{exp}}\right]^2}{N-P}} \times 100 \quad (11)$$

$$SD = \sqrt{\frac{1}{N-1}\sum_{i=1}^{N}\left(\left|\frac{\bar{q}_{exp\,(i)} - \bar{q}_{cal\,(i)}}{\bar{q}_{exp\,(i)}}\right| - ARRE\right)^2} \quad (12)$$

Thermodynamic Parameters

Variables such as ΔG, ΔH and ΔS were calculated and interpreted using Equations (13)-(17). For the other parameters, R represents the molar gas constant (8.314 J mol^{-1} K^{-1}), and T is the equilibrium temperature (Kelvin).

$$\Delta G = -RT ln\ K \quad (13)$$

$$ln\ K = \frac{\Delta G}{-RT} \quad (14)$$

$$ln\ K = -\frac{\Delta H}{RT} + \frac{\Delta S}{R} \quad (15)$$

$$ln\ K = -\frac{\Delta G}{RT} = \frac{-\Delta H}{RT} + \frac{\Delta S}{R} \quad (16)$$

$$\Delta G = \Delta H + T\Delta S \quad (17)$$

Statistical Analysis

The impact of temperature and extraction time on the rate of extract recovery was analysed using SPSS (Version 21) and determined based on F-values and *P*-values. ANOVA was used to compare the statistical difference between and within groups, and Tukey's post hoc HSD was used to calculate the minimum difference between group means.

RESULTS AND DISCUSSION

Extract Yield

This study found that extract yields were recovered at temperatures ranging from 40°C-80°C and extraction times from 30-150 min as shown in *Table 2*. The initial rate of extract recovery was low at all temperatures, but higher recoveries were seen with longer extraction time (150 min) across all temperatures. The highest and lowest yields were recovered at 40°C, 30 min, and 80°C, 150 min, at 2.61% and 3.95% respectively, indicating a positive relationship between increased time, temperature and extract recovery rate. Kinetically, a forward reaction is driving the recovery rate as yields increase linearly with rising temperature and increasing extraction time. This trend was previously reported by Mgoma *et al*. (2021) in their study of avocado oil extraction using the Soxhlet method. At the initial extraction (30 min), there was a 0.21% difference in yield between 40°C and 80°C, but a significantly higher difference of 0.74% was seen at the final extraction time of 150 min, implying that prolonging the extraction time leads to higher extract recovery. This observation was supported by the work of Baldino *et al*. (2018) and Mohammad and Arami, (2009), who found that longer extraction time leads to greater solubility and higher extract recovery due to increased interaction between the analyte and the extractive solvent (CO_2).

The rate and yield of palm oil extraction increase with temperature as shown in *Figure 2*. A 0.60% difference in yield was observed at the lowest temperature (40°C) between the initial (30 min) and final extraction time (150 min). At the optimum temperature (80°C) during the same time range, a 1.13% difference was obtained. The higher yields at higher temperatures are due to improved solute mass transfer, as supported by the theory of SFE (Mahmoodi *et al*., 2010; Souza *et al*., 2019). The extract yield of 2.61%-3.95% obtained in this work is considerably higher as per extract recovered from non-polar compounds using SCO_2 extraction (Bello *et al*., 2021; Silva *et al*., 2016). Perhaps, this must be connected to the greater molecular interactions between the polar compounds present in the palm fruit peel extracts (carotenoids) and the non-polar SCO_2, which utterly dissolves the compounds due to the similarity law of like dissolve-like since the carotenoids are non-polar (Garcia-Mendoza *et al*., 2015).

TABLE 2. RESULTS OF THE RECOVERED EXTRACTS AT DIFFERENT TEMPERATURES OVER TIME

	Temperature (°C)				
Time (min)	**40**	**50**	**60**	**70**	**80**
30	2.61	2.65	2.68	2.71	2.82
60	2.72	2.78	2.85	3.00	3.18
90	2.90	3.15	3.41	3.57	3.63
120	3.15	3.41	3.68	3.76	3.82
150	3.21	3.50	3.75	3.84	3.95

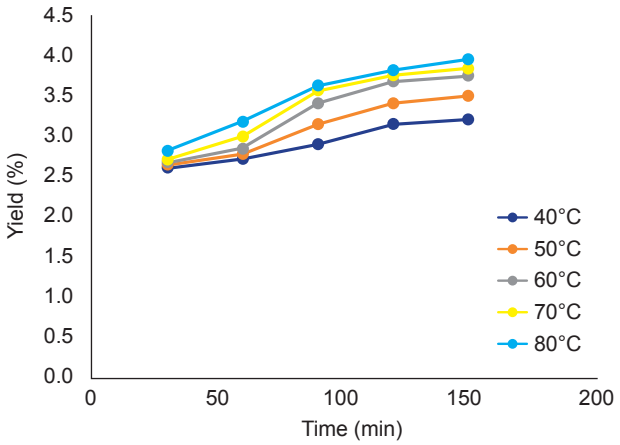

Figure 2. Impact of extraction time and temperature on the recovered oil extract yield.

Kinetic Analysis and Extent of the Models' Fitness

Table 3 presents the model's parameters and the various error estimates calculated using Equations (2)-(12). For the initial and equilibrium oil adsorbed concentrations (E_0 and E_1) of Elovich's model, E_0 decreases as the temperature increases while an increase over temperature rise was seen across the E_1 values except for a sharp decrease at maximum temperature (80°C). Similarly, there is a relative increase in the value of R^2, with the maximum (0.982) obtained at the highest temperature. This suggests that the model supported forward reaction considering the yield increment over temperature rise (Bello *et al*., 2023; Mahmoodi, 2014). However, the calculated R^2, C_1 and C_2 values of the Hyperbolic model show an irregular pattern, such that C_1 and C_2 decrease upon an increase in temperature except at the maximum temperature. This implies that the extraction rate at the initial and final stages of the process are not the same according to the model. For the pseudo-second-order model, the values for the extraction capacity, *Cs* increases as the temperature rises. This confirms that higher temperature resulted in greater extraction capacity due to improving solute mass transfer into the plant matrices. This observation was in close agreement with the findings reported by Gadkari and Balaramanl, (2017). Unlikely, the extraction rate constant, *K* values show an indefinite pattern across the temperatures. Therefore, the higher *K* value (0.0211) obtained at the lowest temperature (40°C), reflects that higher density and diffusion rate at low temperatures resulted in a higher extraction rate (Mahmoodi *et al*., 2019).

TABLE 3. MODELS' PARAMETERS AND ERROR ANALYSIS VALUES FOR THE STUDIED MODELS'

Temperature (°C)	**40**	**50**	**60**	**70**	**80**
Elovich's Model					
E_0	1.2230	0.6260	0.0720	0.0500	0.2830
E_1	0.3880	0.5670	0.7340	0.7630	0.7330
R^2	0.9110	0.9220	0.9190	0.9530	0.9820
RMS	0.0244	0.0332	0.0428	0.0310	0.0176
SEE	0.0282	0.0382	0.0505	0.0393	0.0231
ARE %	0.1029	0.0620	0.1010	0.0713	0.0405
SSE	0.0238	0.0438	0.0765	0.0462	0.0159
HYBRID %	0.1715	0.1034	0.1684	0.1189	0.0675
MPSED %	3.1516	4.2852	5.5238	4.0058	2.2729
SD	0.0021	0.0019	0.0030	0.0021	0.0008
Hyperbolic Model					
C_1 (min^{-1})	0.3897	0.2952	0.2455	0.2395	0.2635
C_2 (min^{-1})	0.1189	0.0812	0.0611	0.0570	0.0617
R^2	0.8000	0.8200	0.8370	0.9080	0.9460
RMS	0.0362	0.0470	0.0561	0.0418	0.0297
SEE	0.0423	0.0565	0.0687	0.0530	0.0400
ARE %	0.2112	0.0155	0.0475	0.0394	0.0195
SSE	0.0536	0.0958	0.1416	0.0843	0.0479
HYBRID %	0.3521	0.0259	0.0791	0.0656	0.0325
MPSED %	4.6422	6.0329	7.2187	5.3946	3.8283
SD	0.0063	0.0005	0.0014	0.0012	0.0006
Pseudo 2nd Order Model					
k ($L\ g^{-1}\ min^{-1}$)	0.0211	0.0133	0.0096	0.0101	0.0110
C_s ($g\ L^{-1}$)	3.4722	3.9216	4.3478	4.4248	4.4643
R^2	0.9950	0.9930	0.9900	0.9940	0.9970
RMS	0.0465	0.0549	0.0606	0.0444	0.0336
SEE	0.0509	0.0610	0.0687	0.0523	0.0408
ARE %	0.5170	0.3814	0.2251	0.1723	0.2806
SSE	0.0777	0.1117	0.1416	0.0822	0.0500
HYBRID %	0.8616	0.6357	0.3751	0.2871	0.4677
MPSED %	6.0014	7.0882	7.8239	5.7350	4.3375
SD	0.0103	0.0076	0.0045	0.0034	0.0056

Models Degree of Comparable Fitness

Figure 3a, *3b* and *3c* show the histograms for the degree of the comparable fitness of the tested models to the experimentally derived data of oil extract. The highest calculated yield of 3.96% and 3.17% was obtained by Elovich's model at 80°C and 40°C respectively after 150 min of extraction (*Figure 3a*). Also, at an initial extraction time of 30 min, the same model gave an extract yield of 2.78% and 2.54% at similar temperatures. Comparatively, at the initial extraction (30 min), it was observed that the difference between the model's calculated and the experimentally obtained yield at 80°C and 40°C are 0.04 (<5%) and 0.07 (>5%) respectively. However, at the final extraction time (150 min), the least difference was observed at 80°C and 40°C, corresponding to 0.01 (1%) and 0.04 (<5%) respectively. These insignificant differences obtained at the boundary temperatures over time indicate the suitability of this model in fitting the experimental data. Moreover, the correctness of the model was further attested by considering the higher average R^2 value of 0.9374 (close to unity) presented by the model (Riahi *et al*., 2017). For the Hyperbolic model (*Figure 3b*), the calculated model's yields were 3.86% and 3.10% after 150 min of extraction at 80°C and 40°C respectively. However, at the initial extraction time (30 min), the model's calculated yield was 2.77% and 2.56% obtained at 80°C and 40°C. The difference between the model calculated and the experimentally obtained yield at the two boundary temperatures (80°C and 40°C) are 0.09 (>5%) and 0.11 (>10%), at the extraction time of 150 min and 30 min respectively.

Unlike the other two models, a significant difference was observed between the experimental data obtained, and the calculated yield presented by the pseudo-second model (*Figure 3c*). However, at the initial time (30 min), a difference of 0.16 (>15%) and 0.22 (>20%) were recorded at the 80°C and 40°C respectively. On the other hand, a much lower difference of 0.02 and 0.03 (<5%) were recorded at 80°C and 40°C respectively after 150 min. Therefore, this wide variance indicates the non-suitability of this model in fitting the experimental data. Consequently, the results of the comparative analysis between the models' calculated and the experimental yields, aligned with that of the kinetic analysis of the error functions. Hence, Elovich's is the most suitable model that best fitted the experimental data owing to its lower error values and least significant difference between the model's calculated and experimental extract yield. This was followed by Hyperbolic and then Pseudo second order respectively.

As shown in *Table 4*, the average values of the statistical error functions, Elovich's model had the lowest average values of the calculated error functions. This was followed by Hyperbolic and then Pseudo 2nd order. However, the highest average R^2 values 0.9938, 0.9374 and 0.8622 were presented by Pseudo second order, Elovich's, and Hyperbolic respectively. This shows that Elovich's is the most suitable model that best fitted the kinetics data since it gave the lowest average values of the tested error parameters. This was followed by Hyperbolic and then Pseudo second order model as shown in *Table 4*. This kinetic pathway was similar to that reported by Bello *et al*. (2023), on the oil extraction and kinetics of banana peel.

Thermodynamic Analysis

The effect of heat energy changes otherwise called the thermodynamic effects associated with the extraction process was studied and the values of the relevant thermodynamic parameters are presented in *Table 5*. Equations (13) and (15), were used in determining the values of the various thermodynamic parameters namely ΔG, ΔH and ΔS. A plot of *ln* K against 1/T (*Figure 4*), produced a straight-line graph that accounts for the changes in enthalpy and entropy, ΔH and ΔS respectively. According to the results, a value of 53.50 K J mol^{-1} was obtained for ΔH. This positive value implies that the process releases heat to the surroundings (endothermic reaction), hence less energy is required to extract the oil from the milled palm fruit sample. Amarante *et al*. (2014) and Riahi *et al*. (2017) reported similar observations in the past following an oil extraction from castor cake and date palm fibres respectively. From the slope and intercept of the thermodynamic plot (*Figure 4*), a value of 0.138 J mol^{-1}K^{-1} was obtained for the ΔS. This positive ΔS value suggests that the extraction of the palm fruit peels reported in this work is a forward reaction. Perhaps, this is justified considering the symmetrical increase in the rate of extract recovery over temperature rise. Furthermore, the values for the ΔG calculated at both temperatures were negative (*Table 5*), indicating that the extraction proceeds independently without energy input from the external source, as such energy is released (Nasrollahi *et al*., 2018).

One-way ANOVA for the Effect of Temperature and Time on the Yield

Table 6 displays the results of ANOVA on the impact of temperature and extraction time on extract yield. The ANOVA found an increase in extract yield with temperature and time, leading to the rejection of the null hypothesis since

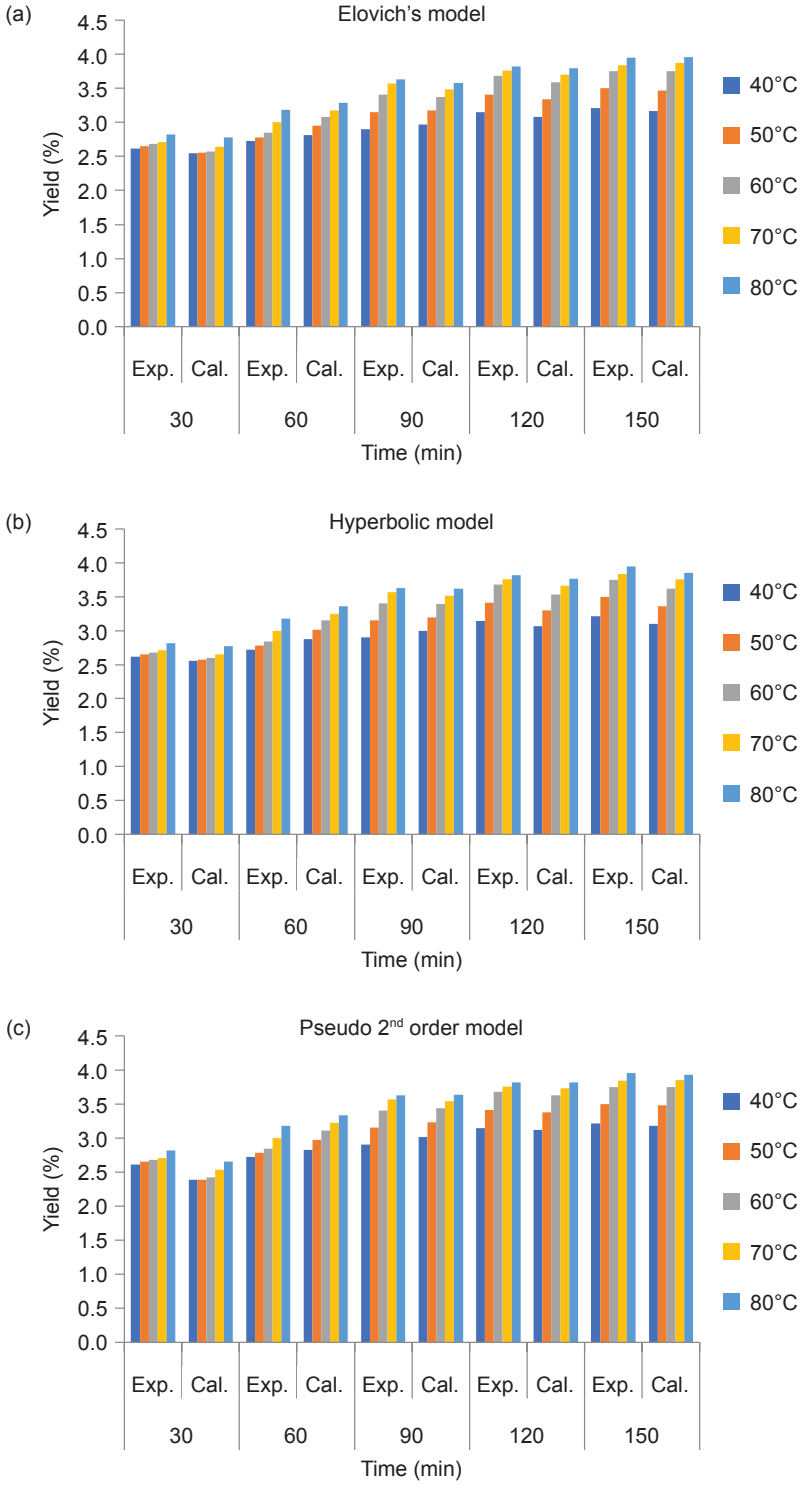

Figure 3. Comparative evaluation of the experimental and models calculated palm fruit extracts for (a) Elovich's, (b) Hyperbolic, and (c) Pseudo 2nd order at different temperatures.

TABLE 4. CALCULATED AVERAGE VALUES OF THE STUDIED ERROR FUNCTIONS

Models	RMS	SEE	ARE	SSE	HYBRID	MPSED	SD
Elovich's	**0.0298**	**0.0359**	0.0755	**0.0412**	0.1259	**3.8479**	**0.0019**
Hyperbolic	0.0422	0.0521	**0.0666**	0.0846	**0.1110**	5.4233	0.0020
Pseudo 2nd order	0.0480	0.0547	0.3153	0.0926	0.5254	6.1972	0.0063

Note: The lowest error values are in bold.

TABLE 5. THERMODYNAMIC PARAMETER FOR PALM FRUIT PEELS EXTRACTION

(K)	K	ΔH KJ mol^{-1}	ΔS KJ mol^{-1}	ΔG KJ mol^{-1}
313	7.86×10^{1}			-11.36
323	2.53×10^{0}			-8.67
333	9.02×10^{0}	53.50	0.138	-6.09
343	8.22×10^{0}			-6.01
353	7.84×10^{0}			-6.04

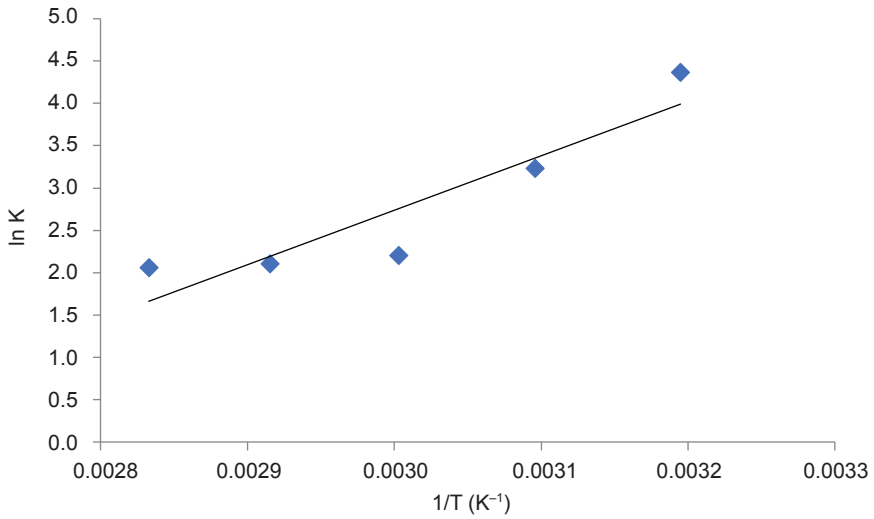

Figure 4. Plot of ln K against 1/T for palm fruit peels.

TABLE 6. ANOVA RESULT FOR THE EFFECT OF THE PROCESS PARAMETERS ON EXTRACT YIELD

Effect of temperature	Sum of squares	DF	Mean squares	F-values	*P*-values	Percentage contribution
Between groups	28.93	4	14.46	91.97	0.000	76.8
Within groups	2.75	25	0.10			
Total	31.68	29				
Effect of extraction time						
Between groups	3.61	4	0.2278	27.78	0.044	23.1
Within groups	1.20	25	0.0874			
Total	4.81	29				

both parameters had *P*-values less than 0.05, indicating statistical differences. To determine significant changes, Tukey's post hoc HSD analysis was performed, as shown in *Tables 7* and *8* for temperature and time respectively, revealing significant differences between performance means. The mean differences marked with an asterisk ($p<0.05$) were considered significant, while those without ($p\geq0.05$) were not. A similar trend was reported by Bello *et al*. (2023) in their study on banana peel extraction. The relative significance of the parameters was also evaluated at 95% confidence using F-values and *P*-values. Hence, the ANOVA results showed that temperature had a higher impact on the rate of extract recovery with an F-value of 91.97, compared to extraction time which had an F-value of 27.78. This means that temperature contributed 76.8% while extraction time contributed 23.1% to the rate of extract recovery. The results suggest that a higher temperature and shorter extraction time resulted in greater extract yield, as it improves solubility, mass transfer and diffusion (Senthilkumar *et al*., 2019). These findings are in line with the data presented in *Table 2*, which shows that higher temperatures result in increased extract recovery.

TABLE 7. EFFECT OF TEMPERATURE ON % YIELD ANALYSED USING TUKEY HSD

Temp. (I)	Temp. (I)	Mean diff (I-J)	Std. error	Sig.	95% confidence level	
					Lower bound	Upper bound
40°C	50°C	2.1920*	0.0882	0.000	2.0109	3.3731
	60°C	1.9080	0.0882	0.101	1.7269	2.0891
	70°C	-2.1920*	0.0882	0.003	-2.3731	-2.0109
	80°C	-0.2840	0.0882	0.052	-1.0199	1.5099
50°C	40°C	-1.9080*	0.0882	0.012	-3.7399	-0.7899
	60°C	0.2840	0.0882	0.050	-1.9099	0.6199
	70°C	2.2320*	0.0882	0.000	-1.9832	0.5466
	80°C	1.9900*	0.0882	0.001	0.7899	1.7399
60°C	40°C	-0.2420*	0.0882	0.000	-1.4349	1.0949
	50°C	-0.0933	0.0882	0.092	0.3660	1.1799
	70°C	-0.2033*	0.0882	0.011	-1.4766	-0.0699
	80°C	-0.3816*	0.0882	0.000	-1.6549	0.8916
70°C	40°C	0.0933*	0.0882	0.000	-1.70116	0.8449
	50°C	-0.1100*	0.0882	0.000	-1.1799	1.3666
	60°C	-0.0460*	0.0882	0.001	-1.9604	0.5170
	80°C	0.2500	0.0882	0.086	2.0787	0.3987
80°C	40°C	-0.8400	0.0882	0.061	-2.1654	0.3120
	50°C	0.9267*	0.0882	0.000	-0.5170	1.9604
	60°C	0.7217*	0.0882	0.000	0.9370	1.5404
	70°C	0.3016*	0.0882	0.000	1.4437	1.0337

Note: *The mean difference is significant at the 0.05 level.

TABLE 8. EFFECT OF TIME ON % YIELD ANALYSED USING TUKEY HSD

Time. (I)	Time. (I)	Mean diff (I-J)	Std. error	Sig.	95% confidence level	
					Lower bound	Upper bound
30 (min)	60 (min)	0.2050	0.6014	0.736	-1.3570	1.1204
	90 (min)	0.8400	0.6014	0.175	-1.4437	1.0337
	120 (min)	0.4200*	0.6014	0.003	-0.3897	2.0787
	150 (min)	0.1183	0.6014	0.846	-0.8187	1.6587
60 (min)	30 (min)	0.2450	0.6014	0.693	-3.7399	-0.7899
	90 (min)	-0.4750	0.6014	0.447	-1.9099	0.6199
	120 (min)	0.6450*	0.6014	0.000	-1.9832	0.5466
	150 (min)	0.7183	0.6014	0.304	-1.9099	0.6199
90 (min)	30 (min)	0.2450	0.6014	0.253	-1.9832	0.5466
	60 (min)	-0.4750*	0.6014	0.001	-0.5448	1.9849
	120 (min)	0.7200	0.6014	0.110	-0.7899	1.7399
	150 (min)	0.1700	0.6014	0.071	-1.4349	1.0949
120 (min)	30 (min)	0.6450	0.6014	0.160	-1.70116	0.8449
	60 (min)	0.1700*	0.6014	0.004	-1.1799	1.3666
	90 (min)	-0.0460*	0.6014	0.000	-1.9604	0.5170
	150 (min)	-0.7333	0.6014	0.086	2.0787	0.3987
150 (min)	30 (min)	0.9633	0.6014	0.129	-0.3016	2.2282
	60 (min)	0.7183*	0.6014	0.002	-0.5466	1.9832
	90 (min)	0.2433	0.6014	0.695	-1.0216	1.5082
	120 (min)	0.0733	0.6014	0.906	-1.1916	1.3382

Note: *The mean difference is significant at the 0.05 level.

CONCLUSION

This work reported the utilisation of a green extraction technique (SFE) to recover liquid extract from palm fruit peels, yielding 3.95% at the highest temperature with a prolonged extraction time. The increase in yield with rising temperature is due to increased diffusivity and solubilisation of the analyte from the plant matrix. The results of the kinetic analysis indicate that the Elovich model is the most suitable for the experimental data due to its lower error values and closest agreement with the experimental data. The Hyperbolic and Pseudo second order models were also evaluated. The significance of extraction time and temperature in improving the rate of extract recovery was confirmed by the ANOVA and Tukey's *post hoc* HSD analysis. Finally, the thermodynamic analysis showed that the extraction process was spontaneous, and that heat is released considering positive values and negative values.

ACKNOWLEDGEMENT

The financial support offered by the HICOE, Centre for Biofuel and Biochemical Research (CBBR), and Yayasan Universiti Teknologi Petronas (Cost Centre of 015MA0-052 and 015LC0-438) is gratefully acknowledged. The support from the Chemical Engineering Department, UTP, and the Centre Graduate Studies, CGS, through the HICoE award to CBBR is duly acknowledged.

REFERENCES

Aini, N; Bello, U; Sya, M and Ruslan, H (2022). The role of antioxidants in improving biodiesel's oxidative stability, poor cold flow properties, and the effects of the duo on engine performance: A review. *Heliyon, 8(7)*: e09846. DOI: 10.1016/j.heliyon.2022.e09846.

Amarante, R C A; Oliveira, P M; Schwantes, F K and Morón-Villarreyes, J A (2014). Oil extraction from castor cake using ethanol: Kinetics and thermodynamics. *Ind. Eng. Chem. Res.*, *53(16)*: 6824-6829. DOI: 10.1021/ie500508n.

Anuar, M A M; Amran, N A and Ruslan, M S H (2021). Optimization of progressive freezing for residual oil recovery from a palm oil-water mixture (POME Model). *ACS Omega*, *6(4)*: 2707-2716. DOI: 10.1021/acsomega.0c04897.

Baldino, L; Della Porta, G; Osseo, L S; Reverchon, E and Adami, R (2018). Concentrated oleuropein powder from olive leaves using alcoholic extraction and supercritical CO_2-assisted extraction. *J. Supercrit. Fluids*, *133(June 2017)*: 65-69. DOI: 10.1016/j.supflu.2017.09.026.

Bello, U; Aini, N and Samsuri, S (2023). Kinetics, thermodynamic studies, and parametric effects of supercritical CO_2 extraction of banana peel wastes. *Sustain. Chem. Pharm.*, *31(December 2022)*: 100912. DOI: 10.1016/j.scp.2022.100912.

Bello, U; Udofia, L; Ibitowa, O A; Abdullahi, A M; Sulaiman, I and Yahuza, K M (2021). Renewable energy transition: A panacea to the ravaging effects of climate change in Nigeria. *J. Geosci. Environ. Prot.*, *09(12)*: 151-167. DOI: 10.4236/gep.2021.912010.

Chai, Y H; Yusup, S; Ruslan, M S H and Chin, B L F (2020). Supercritical fluid extraction and solubilization of *Carica papaya* Linn. leave in a ternary system with CO_2 + ethanol solvents. *Chem. Eng. Res. Des.*, *156*: 31-42. DOI: 10.1016/j.cherd.2020.01.025.

Chanioti, S; Katsouli, M and Tzia, C (2021). Novel processes for the extraction of phenolic compounds from olive pomace and their protection by encapsulation. *Molecules*, *26(6)*: 56-65. DOI: 10.3390/molecules26061781.

da Silva, R P F F; Rocha-Santos, T A P and Duarte, A C (2016). Supercritical fluid extraction of bioactive compounds. *TrAC - Trends in Analytical Chemistry*, *76*: 40-51. DOI: 10.1016/j.trac.2015.11.013.

Gadkari, P V and Balaramanl, M (2017). Mass transfer and kinetic modelling of supercritical CO_2 extraction of fresh tea leaves (*Camellia sinensis* L.). *Braz. J. Chem. Eng.*, *34(3)*: 799-810. DOI: 10.1590/0104-6632.20170343s20150545.

Garcia-Mendoza, M P; Paula, J T; Paviani, L C; Cabral, F A and Martinez-Correa, H A (2015). Extracts from mango peel by-product obtained by supercritical CO_2 and pressurized solvent processes. *LWT*, *62(1)*: 131-137. DOI: 10.1016/j.lwt.2015.01.026.

Mahmoodi, N M (2014). Synthesis of magnetic carbon nanotube and photocatalytic dye degradation ability. *Environ Monit Assess (December)*. DOI: 10.1007/s10661-014-3805-7.

Mahmoodi, N M; Hayati, B; Arami, M and Mazaheri, F (2010). Single and binary system dye removal from colored textile wastewater by a dendrimer as a polymeric nanoarchitecture: Equilibrium and kinetics. *J. Chem. Eng. Data*, *78*: 4660-4668.

Mahmoodi, N M; Taghizadeh, A and Taghizadeh, M (2019). Surface modified montmorillonite with cationic surfactants: Preparation, characterization, and dye adsorption from aqueous solution. *J. Environ. Chem. Eng.*, *7(4)*: 103243. DOI: 10.1016/j.jece.2019.103243.

Meijaard, E; Brooks, T M; Carlson, K M; Slade, E M; Garcia-Ulloa, J; Gaveau, D L A; Lee, J S H; Santika, T; Juffe-Bignoli, D; Struebig, M J; Wich, S A; Ancrenaz, M; Koh, L P; Zamira, N; Abrams, J F; Prins, H H T; Sendashonga, C N; Murdiyarso, D; Furumo, P R and Sheil, D (2020). The environmental impacts of palm oil in context. *Nature Plants*, *6(12)*: 1418-1426. DOI: 10.1038/s41477-020-00813-w.

Mgoma, S T; Basitere, M and Mshayisa, V V (2021). Kinetics and thermodynamics of oil extraction from South Africa hass avocados using hexane as a solvent. *S. Afr. J. Chem. Eng.*, *37*: 244-251. DOI: 10.1016/j.sajce.2021.06.007.

Miękus, N; Iqbal, A; Marszałek, K; Puchalski, C and Świergiel, A (2019). Green chemistry extractions of carotenoids from *daucus carota* L.-Supercritical carbon dioxide and enzyme-assisted methods. *Molecules*, *24(23)*: 1-20. DOI: 10.3390/molecules24234339.

Mohajershojaei, K; Mahmoodi, N M and Khosravi, A (2015). Immobilization of laccase enzyme onto titania nanoparticle and decolorization of dyes from single and binary systems. *Biotechnol. Bioprocess Eng.*, *20(1)*: 109-116. DOI: 10.1007/s12257-014-0196-0.

Mohammad, N and Arami, M (2009). Numerical finite volume modeling of dye decolorization using immobilized titania nano-photocatalysis. *J. Chem. Eng.*, *146(2)*: 189-193. DOI: 10.1016/j.cej.2008.05.036.

Mohammad, N; Arami, M and Yousefi, N (2007). Nanophotocatalysis using immobilized titanium dioxide nanoparticle. Degradation and mineralization of water containing organic pollutant: A case study of Butachlor. *Mater. Res. Bull.*, *42*: 797-806. DOI: 10.1016/j.materresbull.2006.08.031.

Mohammad, N; Oveisi, M; Bakhtiari, M; Hayati, B; Akbar, A; Bagheri, A and Rahimi, S (2019). Environmentally friendly ultrasound-assisted synthesis of magnetic zeolitic imidazolate framework - Graphene oxide nanocomposites and pollutant removal from water. *J. Mole. Liq.*, *282*: 115-130. DOI: 10.1016/j.molliq.2019.02.139.

Nasrollahi, N; Aber, S; Vatanpour, V and Mohammad, N (2018). The effect of amine functionalization of CuO and ZnO nanoparticles used as additives on the morphology and the permeation properties of polyethersulfone ultrafiltration nanocomposite membranes. *Composites Part B*, *154(September)*: 388-409. DOI: 10.1016/j.compositesb.2018.09.027.

Patidar, K; Singathia, A; Vashishtha, M; Kumar Sangal, V and Upadhyaya, S (2022). Investigation of kinetic and thermodynamic parameters approaches to non-isothermal pyrolysis of mustard stalk using model-free and master plots methods. *Mater. Sci. Energy Technol.*, *5*: 6-14. DOI: 10.1016/j.mset.2021.11.001.

Riahi, K; Chaabane, S and Thayer, B Ben. (2017). A kinetic modeling study of phosphate adsorption onto *Phoenix dactylifera* L. date palm fibers in batch mode. *J. Saudi Chem. Soc.*, *21*: S143-S152. DOI: 10.1016/j.jscs.2013.11.007.

Rodrigues, J S; do Valle, C P; Uchoa, A F J; Ramos, D M; da Ponte, F A F; Rios, M A de S; de Queiroz Malveira, J and Pontes Silva Ricardo, N M (2020). Comparative study of synthetic and natural antioxidants on the oxidative stability of biodiesel from Tilapia oil. *Renew. Energ.*, *156(13)*: 1100-1106. DOI: 10.1016/j.renene.2020.04.153.

Ruslan, M S H; Idham, Z; Nian Yian, L; Ahmad Zaini, M A and Che Yunus, M A (2018). Effect of operating conditions on catechin extraction from betel nuts using supercritical CO_2-methanol extraction. *Sep. Sci. Technol. (Philadelphia)*, *53(4)*: 662-670. DOI: 10.1080/01496395.2017.1406947.

Senthilkumar, C; Krishnaraj, C; Sivakumar, P and Sircar, A (2019). Statistical optimization and kinetic study on biodiesel production from a potential non-edible bio-oil of wild radish. *Chem. Eng. Commun.*, *206(7)*: 909-918. DOI: 10.1080/00986445.2018.1538973.

Souza, M E A O; Mezzomo, N; Correa, L C; Lima, M S; Azevêdo, L C and Ferreira, S R S (2019). Recovery of antioxidant compounds from mango peel by green extraction processes. *Int. Food Res. J.*, *26(2)*: 1845-1859.

Valdivia-Rivera, S; Herrera-Pool, I E; Ayora-Talavera, T; Lizardi-Jiménez, M A; García-Cruz, U; Cuevas-Bernardino, J C; Cervantes-Uc, J M and Pacheco, N (2021). Kinetic, thermodynamic, physicochemical, and economical characterization of pectin from Mangifera indica L. cv. Haden residues. *Foods*, *10*(9). DOI: 10.3390/foods10092093.

Vélez-Erazo, E M; Pasquel-Reátegui, J L; Dorronsoro-Guerrero, O H and Martínez-Correa, H A (2021). Phenolics and carotenoids recovery from agroindustrial mango waste using microwave-assisted extraction: Extraction and modeling. *J. Food Process Eng.*, *44(9)*. DOI: 10.1111/jfpe.13774.

Yang, G; Zhao, Y; Feng, N; Zhang, Y; Liu, Y and Dang, B (2015). Improved dissolution and bioavailability of silymarin delivered by a solid dispersion prepared using supercritical fluids. *Asian J. Pharm. Sci.*, *10(3)*: 194-202. DOI: 10.1016/j.ajps.2014.12.001.